Radiology

State of the Art: Clinical Applications of Cardiac T1 Mapping[1]

Erik B. Schelbert, MD, MS
Daniel R. Messroghli, MD

Online SA-CME
See www.rsna.org/education/search/ry

Learning Objectives:

After reading the article and taking the test, the reader will be able to:

- Discuss the advantages of T1 mapping over T1-weighted imaging in cardiac MR imaging
- Explain the concepts underlying the assessment of extracellular volume (ECV) using T1 mapping
- Discuss the diagnostic value of native T1 and ECV in various myocardial diseases

Accreditation and Designation Statement

The RSNA is accredited by the Accreditation Council for Continuing Medical Education (ACCME) to provide continuing medical education for physicians. The RSNA designates this journal-based SA-CME activity for a maximum of 1.0 *AMA PRA Category 1 Credit*™. Physicians should claim only the credit commensurate with the extent of their participation in the activity.

Disclosure Statement

The ACCME requires that the RSNA, as an accredited provider of CME, obtain signed disclosure statements from the authors, editors, and reviewers for this activity. For this journal-based CME activity, author disclosures are listed at the end of this article.

While cardiovascular magnetic resonance (MR) has become the noninvasive tool of choice for the assessment of myocardial viability and for the detection of acute myocardial edema, cardiac T1 mapping is believed to further extend the ability of cardiovascular MR to characterize the myocardium. Fundamentally, cardiovascular MR can improve diagnosis of disease that historically has been challenging to establish with other imaging modalities. For example, decreased native T1 values appear highly specific to detect and quantify disease severity related to myocardial iron overload states or glycosphingolipid accumulation in Anderson-Fabry disease, whereas high native T1 values are observed with edema, amyloid, and other conditions. Cardiovascular MR can also improve the assessment of prognosis with parameters that relate to myocardial structure and composition that complement the familiar functional parameters around which contemporary cardiology decision making revolves. In large cohorts, extracellular volume fraction (ECV) has been shown to quantify the full extent of myocardial fibrosis in noninfarcted myocardium. ECV may predict outcomes at least as effectively as left ventricular ejection fraction. This uncommon statistical observation (of potentially being more strongly associated with outcomes than ejection fraction) suggests prime biologic importance for the cardiac interstitium that may rank highly in the hierarchy of vast myocardial changes occurring in cardiac pathophysiology. This article presents current and developing clinical applications of cardiac T1 mapping and reviews the existing evidence on their diagnostic and prognostic value in various clinical conditions. This article also contextualizes these advances and explores how T1 mapping and ECV may affect major "global" issues such as diagnosis of disease, risk stratification, and paradigms of disease, and ultimately how we conceptualize patient vulnerability.

© RSNA, 2016

In this article, we present current and developing clinical applications of cardiac T1 mapping and review existing evidence on their diagnostic and prognostic value in various clinical conditions. This article also contextualizes these advances and explores how T1 mapping and extracellular volume fraction (ECV) may affect major "global" issues such as diagnosis of disease, risk stratification, and paradigms of disease, and ultimately how we conceptualize patient vulnerability.

Basic Concepts behind Cardiac T1 Mapping

T1 Mapping versus T1-weighted MR Imaging

Due to its underlying physics, magnetic resonance (MR) imaging provides excellent contrast of soft tissues to characterize not only myocardial function,

Essentials

- Cardiac T1 mapping quantifies intrinsic pathologic processes involving the myocardium by using native (precontrast) T1 measures and extracellular volume fraction (ECV) measures.

- Changes in native myocardial T1 may occur with disease affecting the intracellular or extracellular component of the myocardium (eg, edema, amyloid, iron or glycosphingolipid infiltration).

- ECV dichotomizes the myocardium into its cellular and interstitial component and reflects disease limited to the interstitium (eg, myocardial fibrosis or amyloidosis).

- T1 and ECV mapping appear to add diagnostic information for diffuse myocardial fibrosis, myocardial inflammation, infiltrative diseases, and storage diseases.

- ECV measures of myocardial fibrosis appear to improve risk stratification and ECV may be an important biomarker of myocardial vulnerability.

but also myocardial structure. When fast MR imaging techniques such as turbo spin echo (TSE or fast spin echo) became available in the late 1990s and enabled the acquisition of electrocardiographically gated images of the heart within acceptable time limits, the door was open to explore the clinical value of this soft-tissue contrast for the detection of diseases of the heart muscle. In 1998, Friedrich et al published their pioneering article on serial assessment of myocarditis using contrast-enhanced MR imaging (2). In their study, 19 patients with acute myocarditis underwent T1-weighted turbo-spin-echo MR imaging before and during the first 9 minutes after a bolus injection of gadopentetate dimeglumine. It could be shown that the signal enhancement in the myocardium divided by that of the skeletal muscle was higher in patients with acute myocarditis compared with that in normal control subjects, and decreased approaching normal in the course of 84 days. While this study stimulated researchers to apply cardiovascular MR to patients with nonischemic heart disease, the value of the T1-weighted approach in individual patients was limited due to the large overlap between normal and abnormal findings (3). One obvious source of variability was the use of the skeletal muscle as a reference signal, as muscle signal intensity can be affected by age, sex, physical activity, and parallel involvement in the underlying viral disease. In T1-weighted cardiovascular MR, the need for a reference tissue arises from the fact that images are displayed in gray scales with arbitrary units that vary between different studies. One way to overcome these arbitrary gray scales is to measure T1 directly, which is done in T1 mapping. Here, multiple raw images are acquired after a radiofrequency pulse that allow for sampling magnetization/signal recovery along the z-axis and calculating the underlying T1 value for every voxel within the field of view (assuming adequate coregistration of raw images). From these

data, a so-called T1 map is displayed in color or gray scale where signal intensity of each pixel directly encodes its T1 value.

With the introduction of modified Look-Locker inversion recovery (MOLLI) in 2004 (4), a pulse sequence became available that allowed for high-resolution cardiac T1 mapping within a single breath hold at clinical field strength (1.5–3 T). By using this method and others that followed (5–8), cardiovascular MR researchers have started to investigate the value of signal quantification for the detection of myocardial disease without the need for noncardiac reference tissues. As T1 mapping can be performed both with and without contrast agents, the spectrum of applications includes and extends that of both nonenhanced and contrast-enhanced cardiovascular MR techniques such as T2-weighted imaging and late gadolinium enhancement (LGE), respectively. Furthermore, the combination of both nonenhanced (native) and contrast-enhanced T1 mapping with hematocrit data allows one to quantify the concentration of the contrast agent within the myocardium to derive the ECV.

Native T1 and ECV to Characterize Myocardial Structure

Native T1 and ECV introduce novel metrics to characterize fundamental disease processes occurring in the myocardium that reflect alterations in tissue composition and structure (Fig 1). Native T1 measures characteristics relate to the entire myocardium, whereas ECV exploits the extracellular nature of contrast material to measure the noncellular space occupied mostly by the
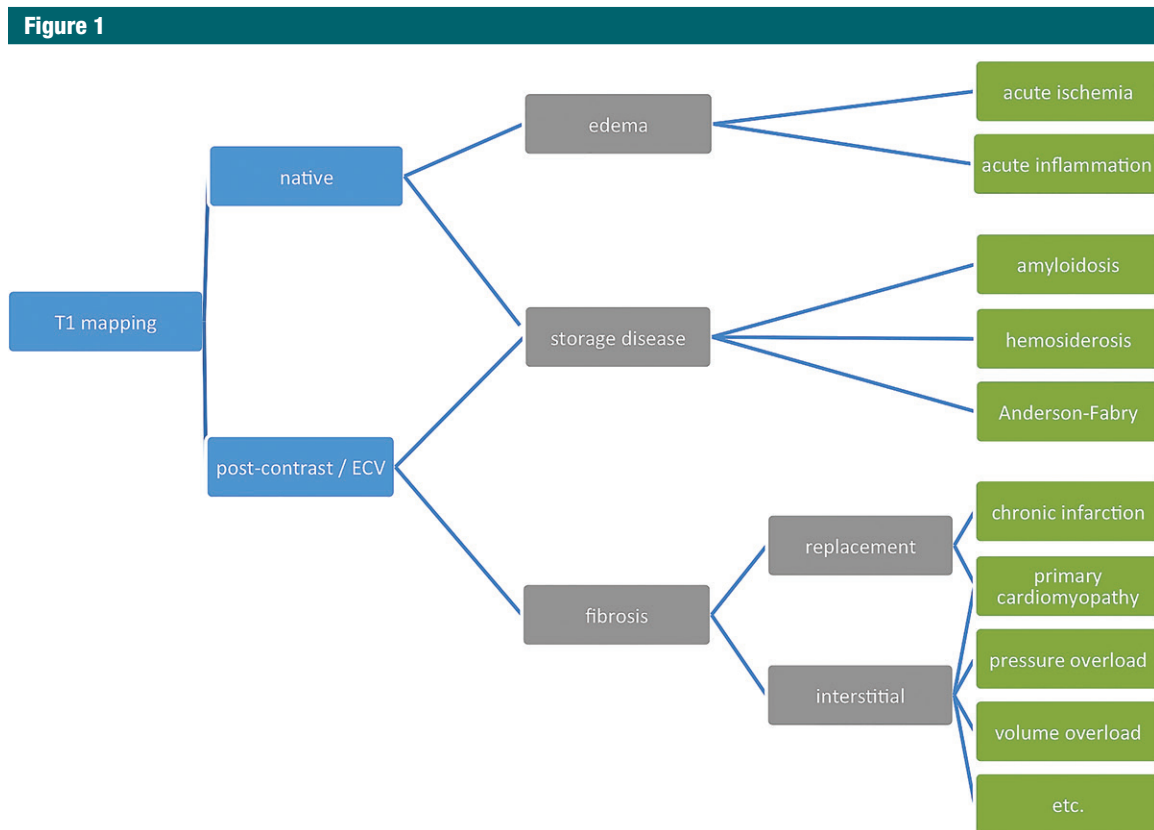
Radiology

Figure 1:   Preferred T1 mapping approaches (blue), mechanisms of tissue injury (gray), and underlying disease (green).

extracellular matrix (ECM) in the interstitium (but ECV also includes the myocardial vasculature). Conceptually, ECV dichotomizes the myocardium into its mostly interstitial (ECV) and cellular (1 − ECV) components.

Myocardial Composition

In normal human myocardium, the cardiomyocyte occupies the majority of the volume (approximately 75%) (9), but these cells constitute only 30%–40% of the total cellular population. The cardiac fibroblast is the most numerous cell in human myocardium and is central to collagen and ECM homeostasis (10). Fibroblasts are widely distributed so that they remain in close proximity to every myocyte. Other cells such as vascular cells (endothelial cells, smooth muscle cells, and pericytes) and the mast cells and macrophages that surround them represent much smaller cell populations (10). Of course, erythrocytes are always in transit through the myocardial vasculature providing oxygen, but their concentration varies across individuals and with the severity of any anemia or polycythemia.

Cardiomyocytes exhibit an ordered laminar arrangement with extensive cleavage planes between muscle layers (approximately 2–6 cells thick) and variation in the coupling between adjacent layers (11). The ECM, composed mostly of fibrillar collagen, provides a three-dimensional network around the myocytes to provide structural support, to transmit forces, and to maintain tissue overall architecture. The epimysium is located on the endocardial and epicardial surfaces, the perimysium surrounds muscle fibers to connect groups of muscle fibers, and the endomysium arises from the perimysium and surrounds individual muscle fibers (10,12). Endomysial struts link muscle fibers and the microvasculature and function as the sites for connections to cardiomyocyte cytoskeletal proteins across the plasma membrane (10). In the absence of cardiac amyloidosis or extracellular myocardial edema, type I fibrillar collagen constitutes most of the ECM and provides rigidity. For this reason, cardiac ECM expansion is often considered synonymous with myocardial fibrosis. Type III collagen confers elasticity and glycosaminoglycans (eg, hyaluronan), glycoproteins, and proteoglycans are also important ECM components (12).

As the most frequently used gadolinium-based contrast media in MR imaging are purely extracellular agents, the T1 shortening that these agents exert on the myocardium is directly linked to their tissue concentration and thus to the volume they occupy in the extracellular space. An exception occurs in specific contrast agents that bind to serum proteins (the concentration of which can vary across patients). In this situation, the contrast agent preferentially distributes away from the intersti-

tium into the vascular space, thus lowering the partition coefficient and biasing ECV measurements downward.

While isolated postcontrast T1 measurements as a surrogate for myocardial ECV have been performed and have been shown to depict alterations in patients with both systolic (13) and diastolic (14) heart failure, the routine use of isolated postcontrast T1 as a biomarker has been discouraged (15) due to its sensitivity to confounders such as changes in contrast agent dose (which is influenced by obesity), time point of postcontrast image acquisition, anemia, and renal function. Instead, the use of ECV is preferable, as ECV avoids these confounders by taking into account the T1 behavior of blood, variable dosing and clearance of the contrast agent, and variation in the hematocrit. ECV measures the volume fraction of the myocardial extracellular space (16,17) and is insensitive to the effects of renal function, anemia/polycythemia, or obesity, all of which are clinically relevant entities in their own right. In the absence of cardiac amyloidosis or extracellular myocardial edema, variation in the extracellular space is determined mostly by the extent of myocardial fibrosis, which has excellent agreement with human histologic measures of the collagen volume fraction with R2 values ranging from 0.7 to 0.9 (18–22). The extent to which ECV is influenced by variation in capillary density or capillary recruitment through variable arteriolar vasodilation is uncertain (23,24) but does not appear to be a major source of variation given the excellent agreement with histologic reference standards. Furthermore, using MR imaging microscopy, gadolinium contrast material appears to track thin strands of collagen with high fidelity at the cellular level (25).

Considerations for Normal T1 Relaxation Times

Under normal conditions, each tissue exhibits T1 (and T2) values within a certain range, that is, some tissues have similar normal T1 values, but a given tissue cannot have completely different T1 values in different normal subjects.

T1 increases with field strength in a nonlinear fashion, that is, native myocardial T1 will be higher at 3 T than at 1.5 T using the same T1 mapping method in the same subject. After administration of a contrast agent, the shortening of T1 directly reflects the concentration of that contrast agent in the tissue of interest, which in turn depends on the dose, the application scheme (eg, bolus, infusion, bolus-infusion protocols), the hematocrit, and the time from application.

Each method for T1 mapping introduces characteristic measurement errors that may influence both accuracy (the ability to yield the true value) and precision (the ability to reproduce the same result in separate measurements) to different degrees. In practice, there is debate about the "true" in vivo reference native T1 values of the myocardium, as the in vitro reference techniques are too lengthy to be applied in vivo, and in vivo conditions (including motion, perfusion, and temperature) cannot be fully reproduced in vitro. Furthermore, many compartments compose the myocardium, such as myocytes, ECM, and the vasculature, which vary in terms of vasodilation, capillary recruitment, and erythrocyte content. These compartments may variably affect T1 measures by different pulse sequences through variable sensitivity to magnetization transfer or water exchange effects that are difficult to reproduce in phantoms in vitro (26,27). Thus, results should always be compared with normal control values that were obtained with the same T1 mapping technique, with the same pulse sequence parameters and at the same field strength (28).

Systematic data on normal behavior are now available for several T1 mapping techniques (8,29–33). In the largest study to date, a subcohort of the MESA trial (Multi-Ethnic Study of Atherosclerosis) comprising 1231 subjects underwent both pre- and postcontrast cardiac T1 mapping (with 1.5-T MR systems from one vendor), from which native myocardial T1 values and ECV were derived (34). The size of this study cohort allowed for detection of

underlying mild age- and sex-specific differences including higher ECV in females and a tiny increase of ECV for both sexes with age.

The situation of pulse sequence dependence is not too problematic. To put the issue into clinical perspective, it resembles that of other important imaging parameters such as left ventricular (LV) ejection fraction, whose normal range also depends on the imaging test and protocol to be used (eg, echocardiography versus MR imaging; long axis versus short axis; spatial and temporal resolution; inclusion or exclusion of trabeculae, papillary muscles, and outflow tract). Since ECV is a ratio of T1 measures analogous to ejection fraction as a ratio of volumes, systematic biases in T1 measures (upwards or downward) can cancel out to some degree to render stable measurements across centers (19,35).

Implementation of Cardiac T1 Mapping in Routine Cardiac MR

Pulse sequences and postprocessing software for cardiac T1 mapping are currently available from all major vendors of MR imaging systems. Typical methods acquire raw data for high-resolution single-section T1 maps of the heart within a single breath hold of the patient and provide online reconstruction of the data with or without motion correction. There are a multitude of techniques and subvariants regarding data acquisition and imaging protocols.

Commonly used cardiac T1 mapping strategies are based on the acquisition of a set of raw images with different degrees of recovery of magnetization along the z-axis following inversion recovery (IR) or saturation recovery (SR) prepulses. These raw images are processed offline (by separate software) (36) or inline (by the image reconstruction engine of the MR imaging system) (37), with or without the use of manual (36) or automatic motion correction (7), to generate voxel-based T1 maps. IR-based approaches include MOLLI (4), shortened MOLLI (called shMOLLI) (5), and variations of the initial 3-3-5 MOLLI scheme, eg, 5-3 MOLLI or 4-3-2 MOLLI (postcontrast imaging). SR-based approaches

Radiology

include SAP-T1 (38) and SASHA (6). Mixed IR-SR approaches such as SAP-PHIRE (39) aim to combine the advantages of IR (higher precision) with those of SR (higher accuracy) (28,40). A detailed description of these technical issues or practical recommendations for imaging protocols are beyond the scope of this work and are addressed further in the Society for Cardiovascular Magnetic Resonance consensus statement on cardiac T1 mapping (15).

Applications Based on Native Myocardial T1

Myocardial Edema

Disease processes within the myocardium usually affect both T1 and T2 values concordantly (prolongation or shortening). A prime example is myocardial edema, which was studied with low-field-strength MR imaging in small and large animal models in the early 1980s (41,42). These studies confirmed previous findings in the brain where the presence of edema led to an increase in both T1 and T2 values, with both properties being directly related to water content. Initially, T2-weighted imaging became the technique of choice for the visualization of edema as the percentage change of T2 in this setting is higher than that of T1 and as water presents as hyperintense on T2-weighted images, whereas on T1-weighted imaging water is hypointense and thus harder to delineate without inverting the image. In parametric MR imaging, where signal intensities reflect relaxation times, higher values will usually be displayed as hyperintense compared with lower values on most scaling algorithms, which is why areas of focal myocardial edema can be delineated as hyperintense areas on both T1 and T2 maps. Thus, both techniques are potential candidates to introduce quantitative signal information to myocardial edema imaging. Both have been shown to accurately delineate the area at risk in a dog model of myocardial ischemia/reperfusion (43). T1 mapping carries the advantage of being combinable with post-contrast application. Whether one or the other provides higher diagnostic accuracy in clinical settings remains to be studied in direct comparison between modern T1 and T2 mapping techniques.

The assessment of myocardial edema is of particular interest as myocardial edema accompanies any acute myocardial injury. While this phenomenon has been known from animal experiments for a long time, MR imaging is the first and until now the only method to directly visualize myocardial edema in clinical patients, which was first demonstrated in a systematic fashion (44) using a T2-weighted (and inversely T1-weighted) short-tau inversion recovery sequence (45,46). Using native T1 mapping in acute myocardial infarction, visual assessment or manual signal-to-noise ratio analysis can be replaced by setting a fixed T1 threshold of three standard deviations above the normal mean. With this approach, myocardial segments with edema can be detected with a sensitivity of 96% and a specificity of 91% (47).

Of particular clinical relevance is the finding that native T1 mapping can also be used to detect myocardial inflammation in patients with acute myocarditis, as the diagnosis of myocarditis remains challenging even with the use of invasive endomyocardial biopsy (48). Ferreira et al recently showed that native T1 mapping yields higher diagnostic accuracy in the detection of myocardial injury due to myocarditis than any T2-weighted approach (49). The authors reported that native T1 values were significantly increased in cases of acute myocarditis and postulated that this phenomenon was most likely due to myocardial edema. The same group found that in the acute setting, the diagnostic accuracy of native T1 mapping was high enough to abstain from the administration of contrast agent (50). Other studies confirmed the superiority of native mapping (both T1 and T2) over conventional cardiac MR techniques except for LGE (51) and suggested that T1 mapping might be able to differentiate between different stages of myocarditis (52). Two studies concordantly found that native myocardial T1 values were also elevated in patients with systemic lupus erythematosus (53,54). Interestingly, this finding did not correlate with the presence or absence of enhancement on LGE images. In patients with rheumatoid arthritis, native T1 and ECV were found to correlate with both myocardial strain and disease activity (55).

Similar to viral myocarditis, myocardial edema is also a typical feature of homograft rejection after heart transplantation. In 1987, Wisenberg et al published their early study on 25 transplant patients who underwent endomyocardial biopsy and both T1 and T2 measurements using a 0.15-T MR system (56). While both myocardial T1 and T2 values were highly prolonged 24 hours after transplantation as compared with normal control subjects, both normalized within 25 days in nonrejecting transplants, but not in grafts with rejection, and were also increased to more than 2 standard deviations of normal in 14 of 15 late rejections. The largest study so far on a modern 1.5-T MR system collected serial cardiac MR and echocardiography data from 22 patients for 20 weeks after transplantation and correlated these noninvasive findings with results from endomyocardial biopsies (57). In this study, T1 and T2 were declining but still significantly elevated as compared with normal myocardium at 20 weeks, and neither T1 mapping nor T2 mapping or peak systolic circumferential strain were able to accurately detect acute allograft rejection in the early phase after heart transplantation.

While the high level of increase in native T1 in acute inflammation clearly favors myocardial edema as the underlying mechanism, T1 changes at later stages might also be attributable to myocardial fibrosis (see below). Whether a comprehensive imaging approach allows for differentiating one from the other is a topic of ongoing experimental and clinical research.

Storage Disease

Native T1 mapping is emerging as an important tool to characterize myocardial tissue directly with presumably

Radiology

more accuracy than nonspecific functional surrogate parameters. These advances are critically important for storage diseases, which have been challenging to demonstrate noninvasively. As outlined above, T1 is governed by several factors including the type and amount of protons within a given voxel, their interactions with the molecular surroundings (eg, ferric iron cations [Fe^{3+}] that are paramagnetic), and the polarity of their covalent bonds (lipid versus water protons). In cardiac amyloidosis, abnormal proteins accumulate within the myocardial interstitial space and significantly alter the composite relaxation time of the tissue. In early studies, segmental T1 measurements (without voxel-based mapping) indicated severe changes of both native (58) and postcontrast (59) T1 values in patients with cardiac amyloidosis. Karamitsos et al performed native T1 mapping in 53 patients with amyloid light chain (AL) amyloidosis and found that myocardial T1 values were significantly elevated compared with those in healthy control subjects even if no cardiac involvement was suspected by clinical and echocardiographic criteria (60). There was no overlap between myocardial T1 values in patients with definite cardiac involvement of amyloidosis and normal control subjects, with T1 values in these patients elevated in the range of 5–10 standard deviations above the normal mean. Interestingly, Fontana and colleagues from the same group could show that native T1 values in patients with transthyretin type amyloidosis (ATTR) were also strongly elevated, but less so than in patients with AL disease (61). This finding was unexpected, as ATTR patients exhibit a higher increase in LV mass than do AL patients. The authors hypothesized that ATTR might possess lower amyloid burden, less hydration of the amyloid, less collagen associated with amyloid, and differential effects on the intracellular signal, or lack other processes from AL such as edema due to light-chain toxicity. Taken together, these two studies showed that native

T1 mapping allows for differentiating patients with cardiac involvement of amyloidosis with high diagnostic accuracy from normal controls and from patients with aortic stenosis or hypertrophic cardiomyopathy, two other conditions causing LV hypertrophy.

Another systemic disease leading to LV hypertrophy is Anderson-Fabry disease. In this rare but underdiagnosed hereditary disorder, a deficiency in the enzyme α-galactosidase A results in the accumulation of glycosphyngolipids within the lysosomes of cells from various organs including cardiomyocytes. Similar to amyloidosis, cardiac involvement indicates a severely impaired prognosis in these patients. However, in contrast to amyloidosis, Anderson-Fabry disease causes shortening of native (precontrast) myocardial T1 values due to the increase in lipid content. Only inferolateral areas present an exception to this finding, as in Anderson-Fabry disease they are frequently affected by midwall enhancement on LGE images, most likely due to focal fibrosis given the increased native T1 value in LGE-positive regions compared with LGE-negative regions (62,63). Reduction of T1 values is detectable in patients with normal wall thickness and becomes more severe in patients with LV hypertrophy (62). In the same study, patients receiving enzyme replacement therapy showed less shortening of myocardial T1 values, hinting at the potential for monitoring disease progression and guiding therapy using T1 mapping.

A second condition causing shortening of T1 is iron overload. Siderotic disease is either due to hereditary hemochromatosis or (more frequently) to repeated blood transfusions for anemia, for example, in thalassemia major. While some patients even with severe hepatic iron overload do not store iron in the heart, those who do are at high risk for heart failure and lethal arrhythmias. Due to its paramagnetic properties, ferric iron exerts strong local alterations of the local magnetic field; the magnitude of these alterations is described by a time constant T2*. The Royal Brompton

group from London showed that T2* mapping allows for the detection and semiquantitative analysis of the iron overload in the heart (64). Moreover the technique is reproducible across different MR systems (65), predicts outcome (66), and can be used to monitor the effects of different pharmacologic therapies. As a result, T2* mapping became the first parametric mapping technique to become a clinical tool and a reference method according to clinical guidelines (67).

Recently, the ability of T1 mapping to assess iron overload was further explored. While T1 is also shortened in the presence of iron, its shortening occurs more linearly and causes less image artifacts than that of T2*, where values can drop from greater than 20 msec in normal myocardium to less than 1 msec in severe cases. This was shown in a study of 106 patients with thalassemia major, which compared the performance of T2*, T2, and T1 mapping, and concluded that both T1 and T2 mapping might be advantageous in patients with low iron content (68). Further work demonstrated that T1 values had superior reproducibility compared with T2* values suggesting that T1 may be a more precise technique for measuring myocardial iron. In addition, a significant proportion of individuals with normal T2* values in fact had low myocardial native T1 values, suggesting a superior sensitivity compared with T2* (69).

Myocardial Fibrosis

Native T1 mapping has been applied to a number of cardiac conditions that lead to diffuse myocardial fibrosis, including arterial hypertension (62); aortic valve stenosis (60,62,70) and regurgitation (71); hypertrophic cardiomyopathy (61,62,72–74); and dilated cardiomyopathy (72,73). Despite the fact that native T1 values reflect the total composite signal of both intra- and extracellular myocardium (other than ECV; see Native T1 and ECV to Characterize Myocardial Structure, above), most studies found a significant increase of myocardial T1 values in cardiac diseases with diffuse myocardial fibrosis as compared

with T1 values in healthy control subjects. Similarly, increased native T1 values have been reported in patients with asymptomatic aortic valve stenosis (75). However, the magnitude of this increase was much lower than that found in myocardial edema (see Myocardial Edema, above) or amyloidosis (see Storage Disease, above) and there was large overlap between diseased and normal groups. Thus, mean native myocardial T1 values provide limited discrimination for diffuse myocardial fibrosis in individual patients. Indeed, in a head-to-head comparison, the remarkably high histologic agreement between collagen volume fraction and ECV was not matched by native T1 measures (19). However, mean myocardial T1 values do not reflect the higher level of inhomogeneity of T1 distribution in these patients. Ongoing research is exploring methods to quantify this T1 inhomogeneity and to evaluate the diagnostic value of such parameters in patients with diffuse myocardial fibrosis.

Post–Gadolinium Chelate Applications and ECV

Replacement Fibrosis and Interstitial Fibrosis

Myocardial fibrosis is a nonspecific final common pathway of disease that may follow any number of cardiac insults (12). Its burden in heart failure appears similar with reduced or preserved ejection fraction (76). Myocardial fibrosis can occur from two fundamentally different cellular pathways involving either cell loss through apoptosis/necrosis with resultant "replacement fibrosis" or primary fibroblast activity without necessarily any myocyte loss with resultant "interstitial fibrosis" (Fig 2). Replacement fibrosis represents the sequelae of *primary myocyte injury* after which collagen synthesis by fibroblasts replaces the void left by necrotic or apoptotic myocytes. LGE can depict macroscopic foci of replacement fibrosis (77,78). In contrast, interstitial fibrosis often represents the sequelae of *primary fibroblast stimulation* without antecedent myocyte

injury, a process usually too diffuse to be detectable at LGE imaging. LGE cannot readily depict diffuse processes unless there is significant heterogeneity, since LGE only depicts regional differences in the distribution of contrast material.

At the cellular level, the degree to which replacement and interstitial fibrosis occur in noninfarcted myocardium is not well understood. Cardiac MR cannot distinguish these processes very well, but ECV usually is measured in noninfarcted myocardium and thus excludes presumably the most common form of replacement fibrosis, myocardial infarction. ECV in noninfarcted myocardium remains prognostically important irrespective of etiology. Regardless of the difficulty distinguishing replacement from interstitial fibrosis in noninfarcted myocardium, one can still draw inference about these processes from the relationship between LV mass and ECV. In myocardial disease characterized primarily by replacement fibrosis, fibrosis and LV mass measures would be expected to correlate inversely. In myocardial disease characterized primarily by interstitial fibrosis, fibrosis and LV mass would be expected to correlate positively.

The clinical distinction between replacement and interstitial fibrosis is further complicated by the fact that both processes can occur simultaneously in the same patient. For example, interstitial fibrosis in noninfarcted myocardium can be observed in ischemic heart disease distinct from the replacement fibrosis clearly occurring in the infarct (79). In fact, noninfarcted myocardium may contain more collagen than the myocardial infarction itself (80). As such, it remains challenging to ascertain whether the etiology of myocardial fibrosis results from replacement fibrosis dominated by myocyte disease or interstitial fibrosis dominated by fibroblast dysfunction (81). Nonetheless, a positive correlation between fibrosis measured by ECV and LV mass has been reported in large cohorts of patients referred for cardiac MR (without evident amyloidosis or hypertrophic cardiomyopathy) (82,83). These cardiac MR observations agree with prior

pathologic observations (84–88) and suggest that interstitial fibrosis is a prevalent and biologically important entity.

The generally positive correlation between mass and fibrosis in noninfarcted myocardium has important implications for the pathophysiology of myocardial fibrosis. Specifically, this finding suggests the potential for a primary role of the myocardial fibroblast in the development of myocardial fibrosis that does not occur solely at the expense of the myocyte compartment (81,89). Indeed, in an elegant proof of concept study, selective and specific activation of myocardial fibroblasts (sparing myocytes) in rodents causes myocardial fibrosis that leads to a heart failure phenotype (90). In addition, the clinical example of cardiac amyloidosis where presumably inert amyloid protein primarily accumulates in the interstitium—specifically *not* as a secondary phenomenon following myocyte injury—illustrates again the direct deleterious consequences of marked ECM expansion, regardless of cause (ie, collagen versus amyloid deposition). In cardiac amyloidosis, severe cardiac dysfunction can ensue, manifest by a pronounced increases in B-type natriuretic peptide and an inexorable deterioration in clinical status with early mortality despite a relatively preserved ejection fraction (91).

LGE versus ECV

LGE is probably the most extensively validated technique for the detection and quantification of myocardial infarction (25,78,92,93). LGE specifically depicts focal differences in myocardial contrast agent concentration from necrosis in the chronic phase and fibrosis in the chronic phase. Importantly, these signal intensity differences are expressed with arbitrary units to depict relative differences among voxels. For myocardial infarction where the differences between normal unenhanced tissue and infarcted enhanced tissue are dramatic and usually well demarcated, this approach works very well. Application of LGE to "nonischemic" replacement fibrosis also permits detection of severe, focal, macroscopic, prognostically relevant replacement
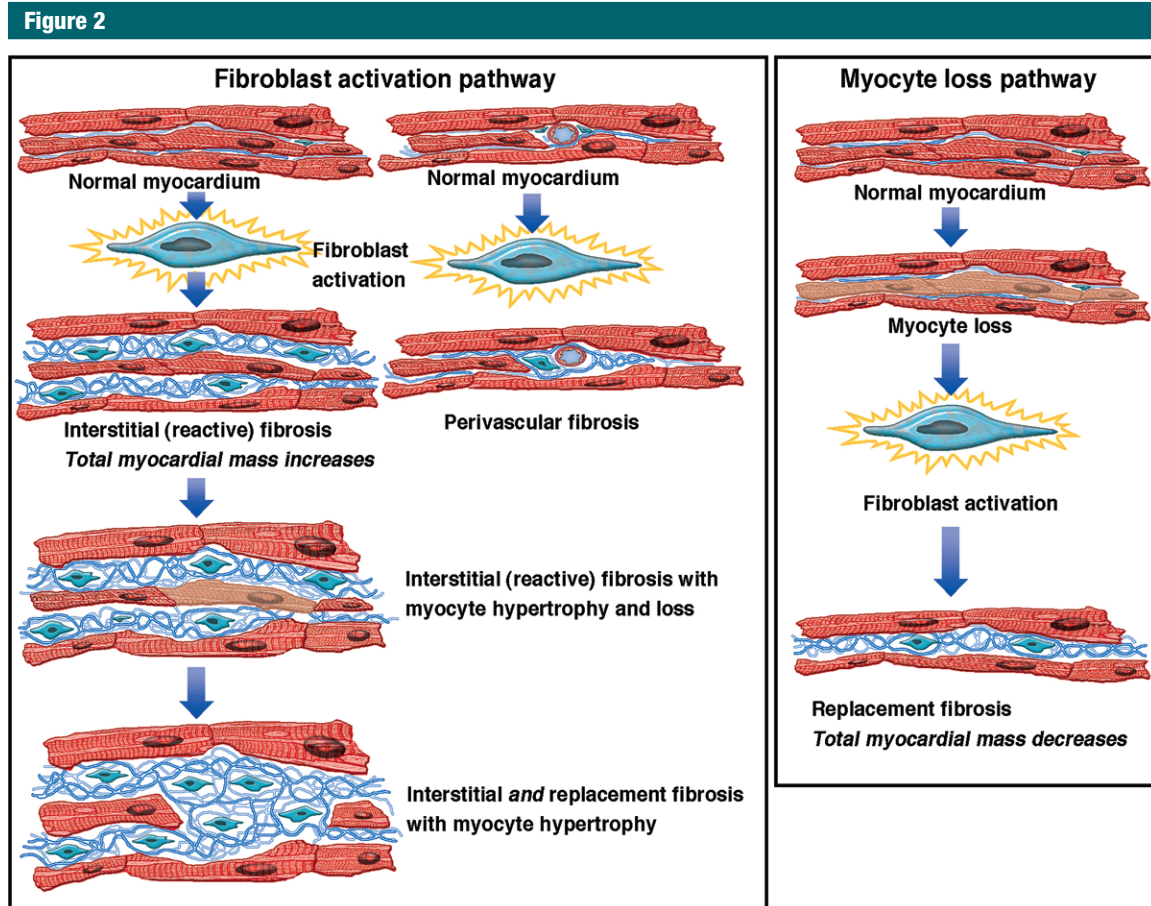
Figure 2: Primary activation of fibroblasts can lead to interstitial fibrosis (left box), and primary myocyte injury can lead to replacement fibrosis (right box). (Reprinted, with permission, from reference 81.)

myocardial fibrosis where there are profound regional differences between areas with and without enhancement on LGE images (77,94–97). For these applications, the distributions of voxel signal intensity between replacement fibrosis and noninfarcted myocardium generally do not overlap, thus permitting its quantification based on the signal intensity expressed in arbitrary units.

Yet, LGE as a technique is not well suited to quantify the full spectrum of fibrosis (15). LGE depends on spatial heterogeneity to display enhancement. Because LGE only shows regional differences, one never knows how much diffuse fibrosis is concealed within nonenhancing myocardium. A focus of fibrosis may be limited to the area with enhancement on LGE images, or it may be "the tip of the iceberg" where LGE

shows only the most severe area of a generalized disease process affecting the myocardium diffusely. LGE can only show focal relative differences in myocardial tissue, and it lacks the ability to depict and quantify diffuse disease. This issue is important because there can be large amounts of fibrosis in noninfarcted myocardium (80,85).

Indeed, myocardial fibrosis exists as a continuous spectrum between focal and diffuse. "Focality" of the fibrosis is the key feature that renders it potentially detectable on an LGE image. Importantly, LGE can erroneously portray nonenhanced myocardium as normal (8,17,18,81,82,98–100) (Figs 3, 4).

In addition, distinguishing lesser degrees of patchy fibrosis from noise on an LGE image remains a common clinical challenge that may depend on a number

of parameters related to the pulse sequence, acquisition parameters, contrast agent dose, coil design, and the patient. Given the inherent challenges of using LGE to quantify the full spectrum fibrosis in noninfarcted myocardium, it is not surprising that the cardiac MR community has not converged on an LGE threshold (eg, full width, half maximum or some number of standard deviations above the mean) to dichotomize "fibrotic" from "nonfibrotic" myocardium. Fundamentally, the notion of a dichotomy is problematic because fibrosis in myocardium exists as a continuum. For this reason, many investigators have embraced ECV as the main measure to quantify the full spectrum of the myocardial fibrosis continuum, since ECV is expressed as a volume percent or proportion of the myocardium.
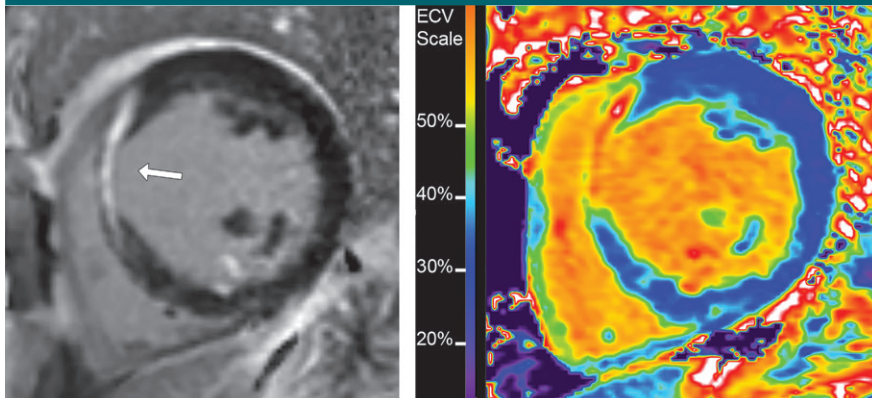
Figure 3

a.   b.

Figure 3: **(a)** LGE imaging data of anteroseptal myocardial infarction in a 60-year-old man shows clear delineation between fibrotic myocardium on LGE image. **(b)** ECV measurement of 25.6% in remote myocardium confirms minimal myocardial fibrosis beyond the infarction.

Figure 4
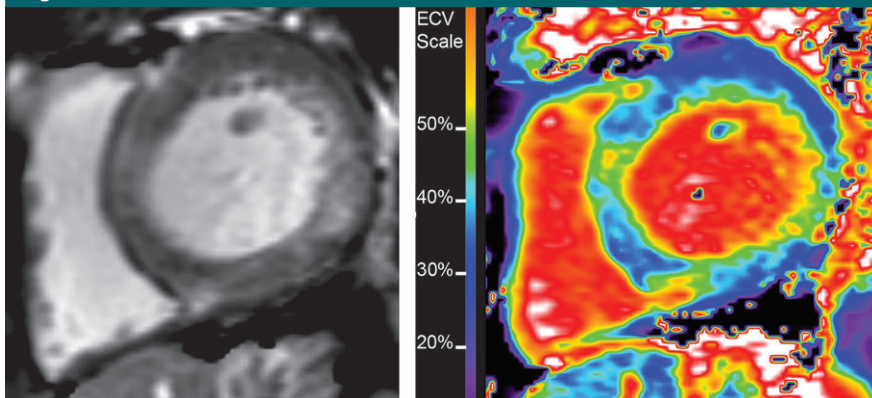

a.   b.

Figure 4: **(a)** LGE imaging data can be ambiguous for ascertaining disease severity in nonischemic fibrosis as shown in this 72-year-old woman with nonischemic cardiomyopathy and poor delineation of fibroitic myocardium on LGE image. **(b)** Yet ECV measures 38.4%, indicating severe diffuse myocardial fibrosis.

The calculation of ECV is based on the observation that the T1 shortening effect of extracellular gadolinium-based contrast agents is directly correlated with their concentration within the extracellular space (Fig 5). When T1 is assessed in myocardium *(myo)* and in blood (usually in the LV cavity) both at the native state and when a steady state of contrast agent distribution *(post-Gd)* between blood and myocardium is reached (which can be assumed 10–15 minutes after administration), given the cellular portion of blood (ie,

the hematocrit which displaces gadolinium-based contrast material) is known, ECV of the myocardium can be calculated with this equation (16):

$$ECV = \frac{\left(\dfrac{1}{T1_{myo\ post-Gd}} - \dfrac{1}{T1_{myo\ native}} \right)}{\left(\dfrac{1}{T1_{blood\ post-Gd}} - \dfrac{1}{T1_{blood\ native}} \right)} \times (1 - hematocrit)$$

The technique in essence measures the myocardial uptake of gadolinium relative to plasma, assuming equilibration of gadolinium-based contrast mate-

rial between extracellular extravascular and intravascular compartments without any intravascular protein binding that would prevent free dispersion of contrast material. The ratio of the relative concentrations in myocardium and whole blood are specifically measured by their change in relaxivity (ie, $\Delta R1 = 1/T1postcontrast - 1/T1precontrast$) to yield the partition coefficient, $\lambda = \Delta R1_{myocardium}/\Delta R1_{blood}$. Since the gadolinium concentration in myocardial interstitial fluid is in equilibrium with plasma (not whole blood), one must correct for the displacement of gadolinium contrast material by erythrocytes and multiply λ by $(1 - hematocrit)$ to yield ECV, which is expressed as a volume percent: $ECV = \lambda \bullet (1 - hematocrit)$. Using appropriate software tools, the calculation of ECV can be performed in a semiautomatic way on a pixel-by-pixel basis to generate ECV maps (Fig 6).

A recent study of patients who underwent renal denervation therapy for resistant arterial hypertension found that at follow-up, myocardial mass was reduced whereas ECV remained unchanged (101). Given the relative nature of ECV (expressed as a volume fraction), it was postulated that the total extracellular volume and thus the total fibrosis load had to be reduced to allow for ECV to remain unchanged in this situation. Hence it might be useful to calculate total extracellular volume (ECV × myocardial volume) in addition to ECV in follow-up studies of patients with LV hypertrophy. Yet, further research is needed to compare total LV mass, total extracellular volume, and ECV in terms of their associations with disease severity measures and outcomes.

ECV measurement is reproducible between cardiac MR studies performed on different days (8,20,102), independent of whether the contrast agent is administered as a single dose or as split bolus injection (103). This translates into fewer subjects required for clinical trials (104). ECV also enables detection of subclinical changes (17,98). Given its high reproducibility, sensitivity, and intrinsically quantitative nature, ECV may be suitable for evaluating serial changes
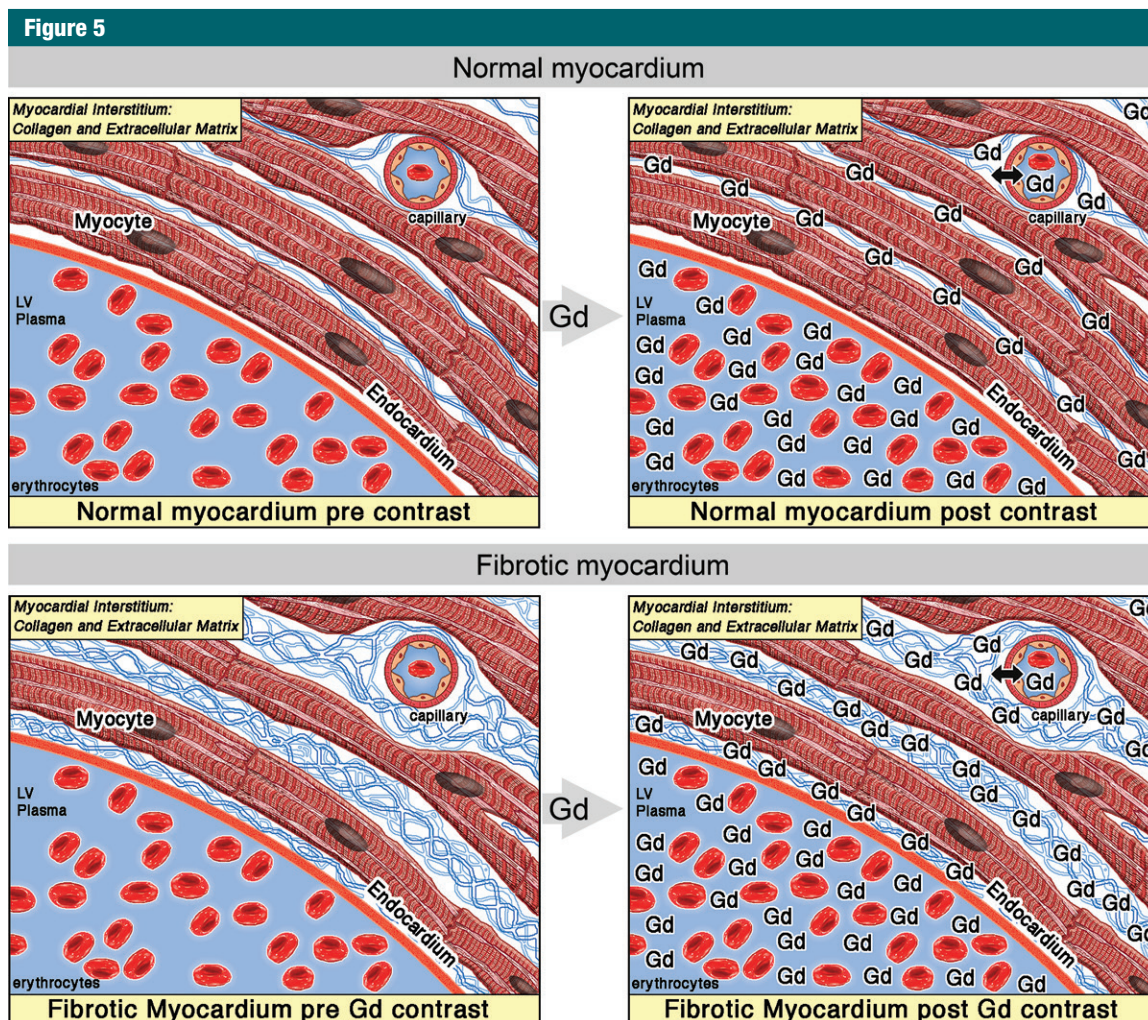
Figure 5

Figure 5: Gadolinium *(Gd)* distribution in myocardium and blood in normal and fibrotic states. The computational steps for ECV measurement are: Step 1, measure *(a)* myocardial and blood pool T1 values before and after extracellular Gd contrast agent administration, and *(b)* the hematocrit. Step 2, compute $\Delta R1$ for myocardium and blood pool where $\Delta R1 = 1/T1_{post\,Gd} - 1/T1_{pre\,Gd}$. Note, $\Delta R1$ linearly relates to the accumulation of Gd in the tissue of interest at a given time point, ie, $\Delta R1 = \gamma \bullet [Gd]$, where γ = the relaxivity of the contrast agent. Step 3, compute λ, the partition coefficient for Gd from the $\Delta R1$ data where $\lambda = \Delta R1_{myocardium}/\Delta R1_{blood\,pool} = [Gd]_{myocardium}/[Gd]_{blood\,pool} = (ECV \bullet [Gd]_{interstitium})/\{(1-hematocrit) \bullet [Gd]plasma\} = ECV/(1-hematocrit)$ if equilibration occurs, where $[Gd]_{interstitium} = [Gd]_{plasma}$. Note, λ "normalizes" the accumulation of (non–protein-bound) Gd in the myocardial interstitium to the concentration of Gd contrast agent in the blood pool after a bolus. Step 4, compute ECV, a unitless measure of the volume fraction of the myocardial interstitium: $ECV = \lambda \bullet (1-hematocrit)$. The $(1-hematocrit)$ term adjusts for key variation in the displacement of Gd contrast agent by the hematocrit which confounds the relationship between ECV and the partition coefficient, λ. (Reprinted, with permission, from reference 81.)

in myocardial fibrosis in noninfarcted myocardium.

Valvular Disease

Most T1 mapping studies on valvular disease have focused on aortic stenosis and demonstrated increased ECV in patients with severe disease (89). However, regurgitant valve disease is of particular interest because of the potential role of diffuse myocardial prognosis in the development of irreversible ventricular remodeling. In a recent study on asymptomatic patients with mitral valve regurgitation it could be shown that ECV correlated with volumetric and functional parameters in these patients (105). Currently studies are underway to assess the value of ECV in determining the optimal time point for valve surgery in both mitral and aortic valve regurgitation.

Congenital Heart Disease

The ability to assess diffuse myocardial fibrosis has attracted a lot of attention from clinicians taking care of patients with congenital heart disease. Primary fields of interest include myocardial injury due to volume overload in pulmo-
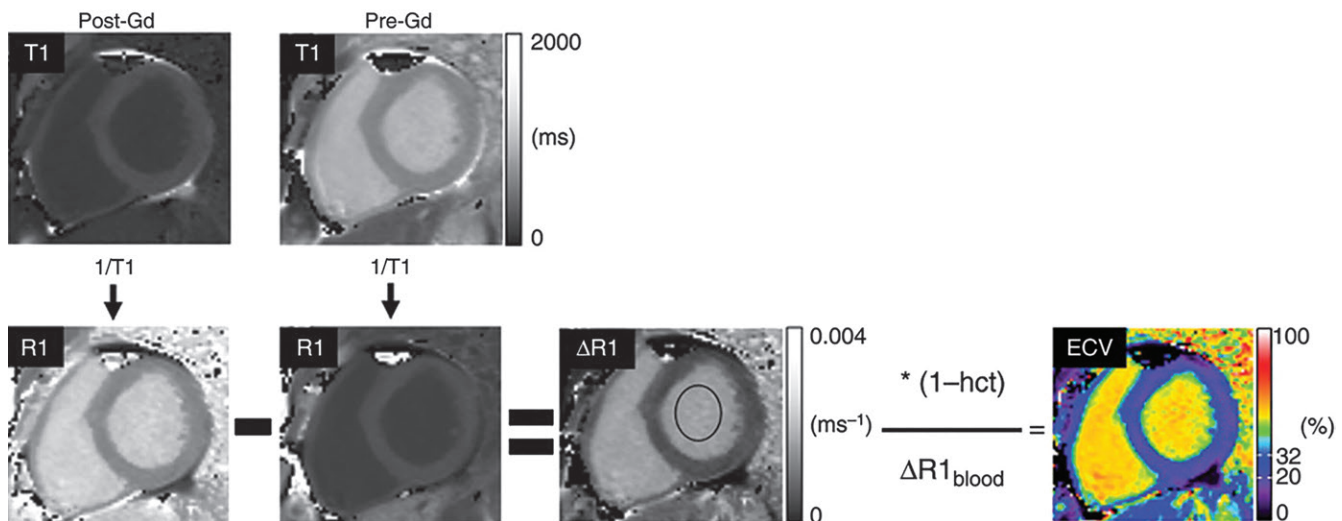
Figure 6

Figure 6: Semiautomatic generation of ECV maps using native and postcontrast (*Pre-Gd* and *Post-Gd*) T1 maps and hematocrit *(hct)*. (Reprinted, with permission, from reference 17.)

nary valve regurgitation (eg, in tetralogy of Fallot), due to pressure overload in systemic right ventricle (congenitally corrected transposition of the great arteries, transposition of the great arteries with previous atrial switch), and due to hypoxemia in cyanotic heart disease (eg, uncorrected ventricular septal defect). Broberg et al found in a series of 50 adult patients with congenital heart disease that ECV was highest in patients with a systemic right ventricle and in those with cyanotic disease (99). These conditions pose specific technical problems for T1 mapping and cardiac MR in general, as they primarily affect the right ventricle, which has thinner walls than the LV (even in cases with severe right ventricular hypertrophy that is less homogeneous than LV hypertrophy) and thus requires imaging with higher spatial resolution. Furthermore, spatial resolution becomes even more critical in pediatric patients. The T1 mapping techniques that are currently most widely used were developed and optimized to provide the best combination of T1 accuracy and spatial resolution within a single breath hold, which is suitable for adult patients with acquired LV heart disease. Patients with right ventricular disease and/or

those of younger age might benefit from non–breath-hold T1 mapping techniques that require a longer acquisition time but provide higher spatial resolution (106).

Storage Disease

Given the distribution of amyloid in the interstitial space, it is not surprising that cardiac involvement in amyloidosis leads to an excessive accumulation of extracellular contrast agents and subsequent marked increase in ECV (107,108). ECV is emerging as an excellent tool to detect and quantify disease severity related to cardiac amyloidosis where the expansion of the myocardial interstitium is especially pronounced. Efforts to validate ECV for this purpose are underway. The substantial shortening of postcontrast myocardial T1 values was initially observed in the first publication on contrast-enhanced cardiac MR in cardiac amyloidosis by Maceira et al in 2005 using nonmapping T1 quantification (59). They noted the irregular behavior of myocardium with amyloid in LGE imaging. In contrast, Anderson-Fabry disease is the prime example of an *intracellular* storage disease that generally spares the extracellular

space. Consequently it was shown that patients with Anderson-Fabry disease do not manifest increased ECV except for regions with additional regional scarring (63).

Chemotherapy-induced Myocardial Injury

Anthracycline therapy, an important element in the treatment of many solid tumors and hematologic malignancies, causes toxic injury to the myocardium through multiple mechanisms (109) and can lead to ventricular dysfunction and heart failure. The degree of myocardial damage depends on individual sensitivity and is further enhanced with increasing cumulative dose. The identification of particularly sensitive individuals before the onset of ventricular dysfunction might help to adjust oncologic therapy at that stage to ameliorate mid- and long-term outcome.

Early studies using nonparametric cardiac MR approaches demonstrated increased myocardial gadolinium uptake after a single course of chemotherapy in individuals who later developed LV dysfunction, demonstrating the potential of contrast-enhanced cardiac MR in this application (110). Published data show that ECV is in-
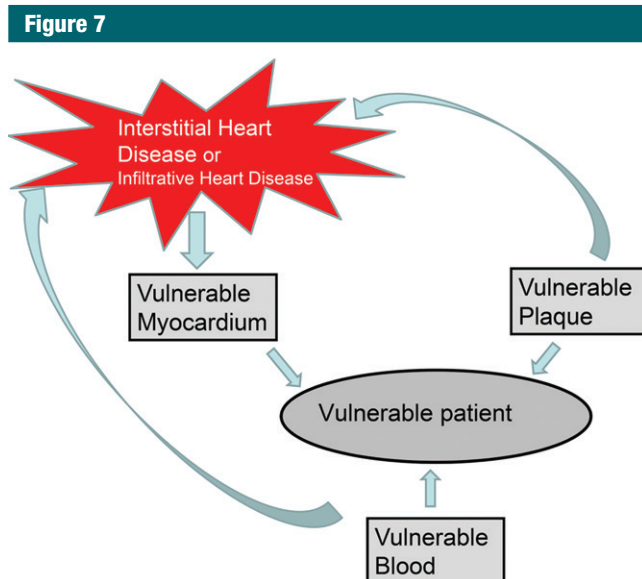
Figure 7

Figure 7: Myocardium, blood, and vascular plaque have been identified as the principal domains underlying patient vulnerability to adverse outcomes. Cardiac MR with T1 mapping and ECV measurement allows one to determine the presence and extent of health or disease in the myocardial domain. For example, infiltrative diseases (ie, amyloid, Anderson-Fabry, and siderosis) and interstitial myocardial disease (usually myocardial fibrosis but also amyloidosis) can be detected and quantified routinely with T1 mapping techniques. Interstitial heart disease in particular indicates myocardial and patient vulnerability to adverse outcomes.

creased in mid- and long-time survivors of anthracycline therapy when compared with normal control subjects. These changes correlate with cumulative dose, impairment of peak oxygen consumption (111), and parameters of diastolic dysfunction (112). Currently, several studies on the acute effect of anthracyclines on myocardial T1 and ECV are underway but results are pending.

Myocardial Inflammation

Given the evidence for increased gadolinium uptake in inflammatory myocardial diseases (viral myocarditis, sarcoidosis, systemic lupus erythematosus) based on conventional MR imaging methods, it can be expected that ECV will be impaired in these conditions. However, there are not enough data on the use of ECV in inflammatory myocardial diseases (53,113) to determine its role in this setting at this point. A key issue is whether suspected increases in

ECV are attributable to inflammation-induced myocardial edema versus myocardial fibrosis. Native T1 data combined with ECV data may be an especially helpful tool to separate these entities.

Myocardial Fibrosis and Paradigms of Vulnerability to Adverse Outcomes

Naghavi et al (136) have previously specified derangement in human myocardium, blood, and vascular plaque as the principal domains underlying patient vulnerability to adverse cardiovascular outcomes (Fig 7). As discussed above, T1 mapping and ECV measurements excel at determining the presence and extent of myocardial health or disease. Infiltrative diseases (ie, amyloid, Anderson-Fabry, and siderosis) and interstitial myocardial disease (usually myocardial fibrosis but also amyloidosis) in particular can be detected and quantified routinely with T1 map-

ping techniques. Interstitial heart disease in the form of myocardial fibrosis or amyloidosis especially indicates vulnerability to adverse outcomes (82,83,91).

Given the historical difficulties of assessing the interstitium quantitatively, little is known about how the interstitium interacts with myocytes to affect myocyte energetics (114). Similarly, little is known about how diseased and vulnerable myocardium may interact with vulnerable plaque or vulnerable blood. For example, pre-existing interstitial fibrosis may increase the lethality of other myocardial insults such as acute myocardial infarction, given its adverse effects of mechanical, vasomotor, and electrical function (115,116).

Recent work from large cohorts (1,82,83) suggests that the interstitium may be a principal determinant of vulnerability, governed more by myocardial fibrosis or amyloidosis in noninfarcted myocardium measured by ECV than a disease classification scheme (eg, dilated cardiomyopathy) (22,117) or a disease "exposure variable" such as aortic stenosis (35,89), diabetes (83), heart failure with or without preserved ejection fraction (14,118) (Fig 8). Indeed, preliminary single-center data suggest that ECV appears to be at least as prognostically powerful a risk factor as LV ejection fraction. Surpassing this prognostic benchmark around which many clinical decisions revolve suggests a central role of myocardial fibrosis in assessing patient vulnerability. Among the multitude of changes that occur in diseased myocardium, myocardial fibrosis may rank highly in the hierarchy these changes and confer vulnerability. Preliminary data also indicate that ECV may reclassify individual patients at risk for death, hospitalization for heart failure, or both, using contemporary statistical metrics (eg, net reclassification improvement, NRI) and significant risk adjustment (119). Conceivably, interstitial heart disease could be a causal "risk factor" and not simply a "risk marker." Indeed, myocardial fibrosis is associated with mechanical, vasomotor, and electrical dysfunction (86,120–126). Notably,
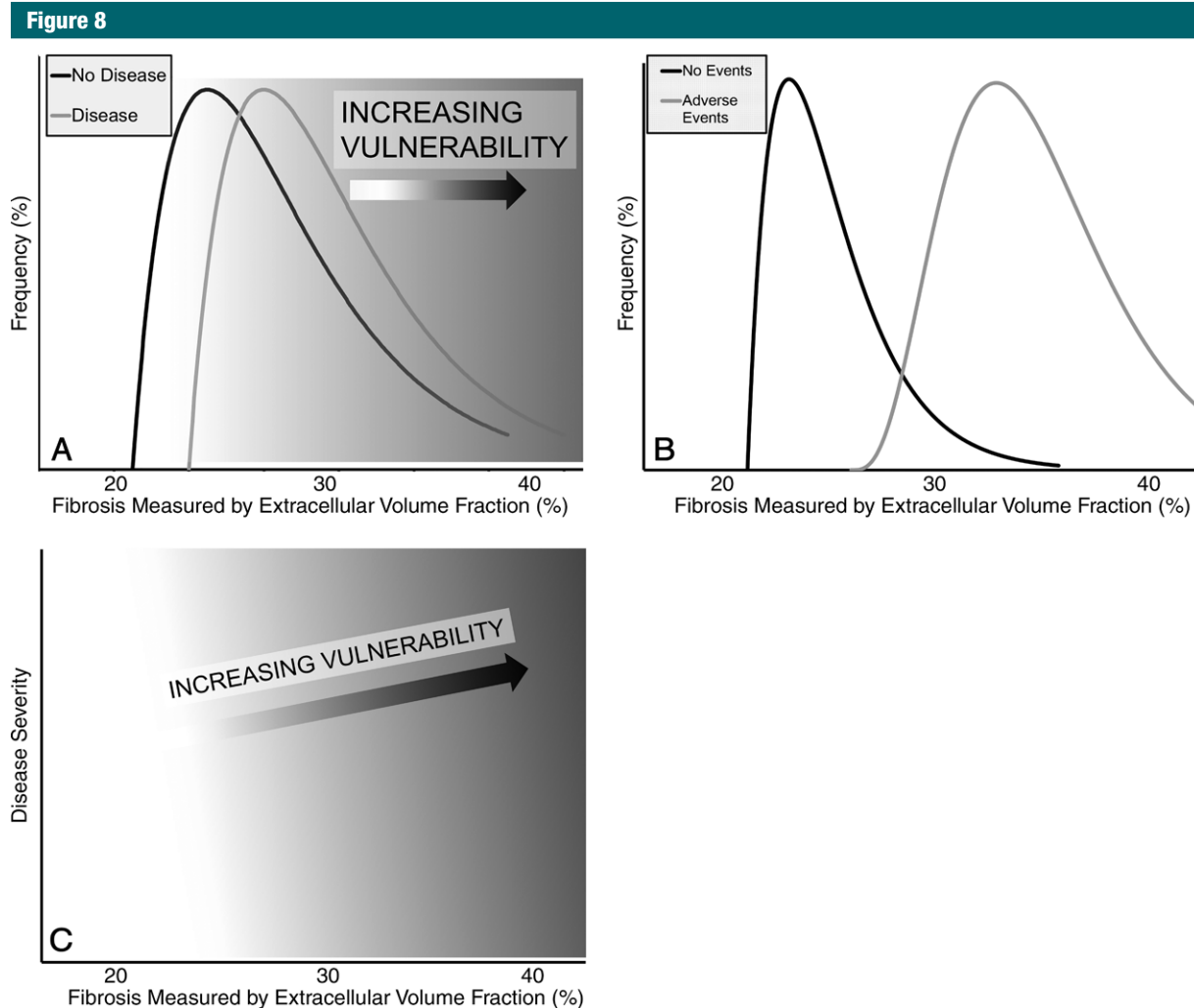
Figure 8

Figure 8: Vulnerability appears to be governed more by myocardial fibrosis measured by ECV than exposure to a particular disease category. Note that the distributions of myocardial fibrosis may exhibit considerable overlap *(A)* between those who are or are not exposed to a given disease state (eg, diabetes, hypertension, aortic stenosis, heart failure with or without preserved ejection fraction). One might falsely assume that this overlap of disease categories limits its clinical assessment of vulnerability, but such an inference is false without ascertainment of subsequent events, which represent the reference standard for vulnerability. Indeed, among those actually experiencing adverse events *(B)*, the separation between ECV distributions is wide (far wider than the disease category in *A*), where most have significantly elevated ECV compared with those who did not experience events. Therefore, myocardial fibrosis response to any given stimulus or disease process may be the critical determinant of vulnerability regardless of a patient's disease category. Chart *C* summarizes these observations and depicts myocardial fibrosis governing vulnerability more than a particular disease exposure.

myocardial fibrosis appears modifiable with resultant improvement of mechanical and vasomotor function accompanying regression of diffuse fibrosis (123–126). Finally, "antifibrotic" treatment with agents that block the renin-angiotensin-aldosterone system improved patient outcomes in several landmark large-scale trials (127–133) in select populations (128).

A common concern arises when ECV distributions overlap between those with and those without a disease state or when ECV distributions overlap according to some disease category. Some may infer that that ECV may not provide clinical and prognostic value because of this overlap. Some may wonder if ECV can only be used to determine the presence or absence of disease at

the population level, but not at the individual patient level. One might then inadvertently assume that this overlap of ECV between disease categories limits its clinical assessment of vulnerability.

We do not share these concerns. It is critical to recognize the current state of ECV data: *(a)* ECV has very strong histologic validation for measuring fibrosis as shown repeatedly by a series of publi-

cations (18–22); *(b)* ECV is highly reproducible between cardiac MR studies performed on different days (8,20,102); and *(c)* ECV can reclassify individual patients at risk for outcomes (119) based on contemporary statistical metrics. In our opinion, these data clearly suggest the potential for use of ECV data in individual patients. We also stress that the role of ECV is not to diagnose the specific disease category for which there is overlap. Rather, ECV can show the extent of fibrosis in individual patients that mostly likely reflects the "fibrotic response" to the various stimuli that govern fibrosis, although regulation of myocardial collagen remains poorly understood. Individuals may be exposed through disease states to conditions that promote fibrosis, yet the fibrotic response across individuals may vary considerably and result in overlapping distributions across disease states.

Ascertainment of subsequent event rates then establishes the associations of any given patient variable with vulnerability. Outcomes data specifically permit one to compare ECV and a given disease category (eg, diabetes) in their strength of association with outcomes. Indeed, with multivariable Cox regression models, we find that elevated ECV confers risk that can be more important *statistically* than the disease category itself (Fig 7). For example, despite the marked overlap of ECV distribution in those with or without diabetes at baseline, the association between ECV and death or hospitalization for heart failure (> 100 events among > 1200 individuals) is approximately threefold higher compared with diabetes based on χ^2 values (unpublished data). Certainly, examining the distributions of ECV reveals a markedly higher ECV in those who experience adverse events compared with those who do not (82). Outcomes are more strongly associated with ECV suggesting the actual fibrotic response of an individual is more prognostically important than that specific disease category which may promote fibrosis inconsistently across individuals.

We propose that the myocardial fibrosis "response" to any given stimulus

or disease process may be the critical determinant of vulnerability, regardless of a patient's disease category, but such knowledge is only apparent by examining subsequent event rates. In general, the stronger the association with outcomes, the more likely the specific measurement is biologically important. Myocardial fibrosis therefore may be an important modifiable therapeutic target for contemporary and emerging treatments (81). Ascertainment of myocardial fibrosis can allow one to assess a patient's vulnerability and allow the clinician to modulate it with antifibrotic therapy. Undoubtedly, more work is needed to understand these emerging issues.

Data regarding the prognostic value of native T1 are limited. Initial reports showing the prognostic ability of native T1 in amyloidosis where native T1 predicted mortality are encouraging (1). Whether disease severity measured by native T1 values of myocardial siderosis or glycosphyngolipid accumulation carries prognostic value in addition to the apparent diagnostic value has not yet been reported.

Limitations of T1 Mapping

A number of issues can compromise T1 and ECV measurements. These have been previously reviewed (15,28). Partial volume effects whereby anisotropic voxels straddle anatomic borders limit the ability of T1 mapping to measure thin structures such as the atria and the right ventricle (15). For this reason, investigators avoid the endocardial and epicardial layers of myocardium when obtaining T1/ECV data. Misregistration of component images that are used to construct the parametric maps is another source of partial volume error. Motion correction techniques with parametric error maps appear important to minimize this problem (7,134,135). In addition, native T1 values appear sensitive to off resonance, heart rate, and specific methodology. ECV calculations, which represent the ratio of T1 values, are less sensitive to systematic biases that are likely to cancel one another in the

mathematical derivation of ECV. Most studies for ECV have reported upper limits of normal in the 25%–30% range, although ECV fundamentally measures a spectrum of disease where the ECV measures reflect the extent of abnormality rendering the dichotomy between normal and abnormal less of an issue. T1 appears sensitive to magnetization transfer effects (26) and ECV exhibits some contrast agent dose/concentration dependence (the tissue concentration of contrast will of course vary with time elapse after a bolus) that may be attributable to water exchange (27). These issues are addressable with careful implementation of methodology (15,28).

Additional issues include different T1 values from different vendors and sites using different methods of T1 mapping. There is no consensus yet on protocol standardization, and it is uncertain whether T1 values obtained with particular pulse sequences are interchangeable across MR imaging machines, which is relevant for multicenter and multivendor studies using T1 mapping data. These factors will be critical to address for broader implementation and utilization of T1 mapping and ECV data. Normalization of native T1 data to a 1000-msec scale and stratification by site for multicenter statistical analyses are some potential solutions to these problems. Despite these pitfalls, T1 mapping and ECV can still stratify patient groups within a center into relevant diagnostic and prognostic categories and fulfill a clinical role.

Similar to a multitude of other cardiac parameters, elevations in native T1 and ECV need to be interpreted within the clinical context. Edema, fibrosis, and amyloidosis can all increase native T1 values and ECV measurements, while low myocardial T1 values appear specific to iron overload or glycosphingolipid accumulation. Because the clinical context is usually known, the clinician may infer whether edema or fibrosis is more clinically likely—for example, an acute chest pain syndrome may favor edema while a chronic cardiomyopathy may favor fibrosis. Amyloidosis appears to cause extreme ele-

vations in native T1 as well as ECV. Given the availability of ancillary clinical data, T1 mapping and ECV still remain promising since they appear to enable detection of important perturbations in myocardial structure. Investigations into the diagnostic and prognostic performance of native T1 remain an active area of research.

Future Role of Cardiac T1 Mapping

Given its incremental diagnostic and prognostic utility to date, cardiac T1 mapping is expected to become an integral part of clinical cardiac MR protocols in patients with known or suspected myocardial disease, which follows a general trend toward quantitative approaches in cardiovascular imaging. The integration of native T1 and ECV measurements into existing protocols for diffuse LV disease is not too burdensome and requires only the assessment of hematocrit (preferably at the time of the examination) and the acquisition of two single–breath-hold T1 maps each before and after the application of an extracellular gadolinium-based contrast agent (15). Typical applications are listed in Figure 1 and include assessment of LV hypertrophy, myocarditis, and overall risk for cardiac events. In general, the major limitation to broad clinical application of this relatively new diagnostic tool is the lack of data from large-scale multicenter trials. With several robust acquisition strategies available, technical aspects have recently become less dominant and there is more emphasis on clinical studies that will hopefully close this gap in information in the field soon. Investigators are laying the foundation to test the hypothesis that cardiac MR-guided care with T1 mapping and ECV improves outcomes.

Conclusion

T1 and ECV mapping appear to be robust, provided care is exercised in their measurement. These cardiac MR techniques can be used to characterize fundamental myocardial structural derange-ments that otherwise may be difficult to detect noninvasively with other modalities. As such, T1 and ECV mapping are emerging as important diagnostic and prognostic tools that could affect the delivery of care and influence paradigms of myocardial disease and the degree of associated vulnerability.

Disclosures of Conflicts of Interest: E.B.S. Activities related to the present article: disclosed no relevant relationships. Activities not related to the present article: disclosed no relevant relationships. Other relationships: author has received MR imaging contrast material from Bracco Diagnostics for research purposes. **D.R.M.** disclosed no relevant relationships.

References

1. Banypersad SM, Fontana M, Maestrini V, et al. T1 mapping and survival in systemic light-chain amyloidosis. Eur Heart J 2015; 36(4):244–251.

2. Friedrich MG, Strohm O, Schulz-Menger J, Marciniak H, Luft FC, Dietz R. Contrast media-enhanced magnetic resonance imaging visualizes myocardial changes in the course of viral myocarditis. Circulation 1998; 97(18):1802–1809.

3. Abdel-Aty H, Boyé P, Zagrosek A, et al. Diagnostic performance of cardiovascular magnetic resonance in patients with suspected acute myocarditis: comparison of different approaches. J Am Coll Cardiol 2005;45(11):1815–1822.

4. Messroghli DR, Radjenovic A, Kozerke S, Higgins DM, Sivananthan MU, Ridgway JP. Modified Look-Locker inversion recovery (MOLLI) for high-resolution T1 mapping of the heart. Magn Reson Med 2004;52(1): 141–146.

5. Piechnik SK, Ferreira VM, Dall'Armellina E, et al. Shortened Modified Look-Locker Inversion recovery (ShMOLLI) for clinical myocardial T1-mapping at 1.5 and 3 T within a 9 heartbeat breathhold. J Cardiovasc Magn Reson 2010;12(1):69.

6. Chow K, Flewitt JA, Green JD, Pagano JJ, Friedrich MG, Thompson RB. Saturation recovery single-shot acquisition (SASHA) for myocardial T(1) mapping. Magn Reson Med 2014;71(6):2082–2095.

7. Xue H, Greiser A, Zuehlsdorff S, et al. Phase-sensitive inversion recovery for myocardial T1 mapping with motion correction and parametric fitting. Magn Reson Med 2013;69(5):1408–1420.

8. Schelbert EB, Testa SM, Meier CG, et al. Myocardial extravascular extracellular vol-ume fraction measurement by gadolinium cardiovascular magnetic resonance in humans: slow infusion versus bolus. J Cardiovasc Magn Reson 2011;13:16.

9. Vliegen HW, van der Laarse A, Cornelisse CJ, Eulderink F. Myocardial changes in pressure overload-induced left ventricular hypertrophy. A study on tissue composition, polyploidization and multinucleation. Eur Heart J 1991;12(4):488–494.

10. Kong P, Christia P, Frangogiannis NG. The pathogenesis of cardiac fibrosis. Cell Mol Life Sci 2014;71(4):549–574.

11. LeGrice IJ, Smaill BH, Chai LZ, Edgar SG, Gavin JB, Hunter PJ. Laminar structure of the heart: ventricular myocyte arrangement and connective tissue architecture in the dog. Am J Physiol 1995;269(2 Pt 2): H571–H582.

12. Weber KT, Brilla CG. Pathological hypertrophy and cardiac interstitium: Fibrosis and renin-angiotensin-aldosterone system. Circulation 1991;83(6):1849–1865.

13. Iles L, Pfluger H, Phrommintikul A, et al. Evaluation of diffuse myocardial fibrosis in heart failure with cardiac magnetic resonance contrast-enhanced T1 mapping. J Am Coll Cardiol 2008;52(19):1574–1580.

14. Mascherbauer J, Marzluf BA, Tufaro C, et al. Cardiac magnetic resonance postcontrast T1 time is associated with outcome in patients with heart failure and preserved ejection fraction. Circ Cardiovasc Imaging 2013;6(6):1056–1065.

15. Moon JC, Messroghli DR, Kellman P, et al. Myocardial T1 mapping and extracellular volume quantification: a Society for Cardiovascular Magnetic Resonance (SCMR) and CMR Working Group of the European Society of Cardiology consensus statement. J Cardiovasc Magn Reson 2013;15(1):92.

16. Arheden H, Saeed M, Higgins CB, et al. Measurement of the distribution volume of gadopentetate dimeglumine at echo-planar MR imaging to quantify myocardial infarction: comparison with 99mTc-DTPA autoradiography in rats. Radiology 1999;211(3): 698–708.

17. Ugander M, Oki AJ, Hsu LY, et al. Extracellular volume imaging by magnetic resonance imaging provides insights into overt and sub-clinical myocardial pathology. Eur Heart J 2012;33(10):1268–1278.

18. Flett AS, Hayward MP, Ashworth MT, et al. Equilibrium contrast cardiovascular magnetic resonance for the measurement of diffuse myocardial fibrosis: preliminary vali-

dation in humans. Circulation 2010;122(2): 138–144.

19. Miller CA, Naish JH, Bishop P, et al. Comprehensive validation of cardiovascular magnetic resonance techniques for the assessment of myocardial extracellular volume. Circ Cardiovasc Imaging 2013;6(3): 373–383.

20. Fontana M, White SK, Banypersad SM, et al. Comparison of T1 mapping techniques for ECV quantification: histological validation and reproducibility of ShMOLLI versus multibreath-hold T1 quantification equilibrium contrast CMR. J Cardiovasc Magn Reson 2012;14:88.

21. White SK, Sado DM, Fontana M, et al. T1 mapping for myocardial extracellular volume measurement by CMR: bolus only versus primed infusion technique. JACC Cardiovasc Imaging 2013;6(9):955–962.

22. aus dem Siepen F, Buss SJ, Messroghli D, et al. T1 mapping in dilated cardiomyopathy with cardiac magnetic resonance: quantification of diffuse myocardial fibrosis and comparison with endomyocardial biopsy. Eur Heart J Cardiovasc Imaging 2015;16(2): 210–216.

23. Jerosch-Herold M, Sheridan DC, Kushner JD, et al. Cardiac magnetic resonance imaging of myocardial contrast uptake and blood flow in patients affected with idiopathic or familial dilated cardiomyopathy. Am J Physiol Heart Circ Physiol 2008;295(3): H1234–H1242.

24. Mahmod M, Piechnik SK, Levelt E, et al. Adenosine stress native T1 mapping in severe aortic stenosis: evidence for a role of the intravascular compartment on myocardial T1 values. J Cardiovasc Magn Reson 2014;16:92.

25. Schelbert EB, Hsu LY, Anderson SA, et al. Late gadolinium-enhancement cardiac magnetic resonance identifies postinfarction myocardial fibrosis and the border zone at the near cellular level in ex vivo rat heart. Circ Cardiovasc Imaging 2010;3(6): 743–752.

26. Robson MD, Piechnik SK, Tunnicliffe EM, Neubauer S. T1 measurements in the human myocardium: the effects of magnetization transfer on the SASHA and MOLLI sequences. Magn Reson Med 2013;70(3): 664–670.

27. Coelho-Filho OR, Mongeon FP, Mitchell R, et al. Role of transcytolemmal water-exchange in magnetic resonance measurements of diffuse myocardial fibrosis in hypertensive heart disease. Circ Cardiovasc Imaging 2013;6(1):134–141.

28. Kellman P, Hansen MS. T1-mapping in the heart: accuracy and precision. J Cardiovasc Magn Reson 2014;16(1):2.

29. Messroghli DR, Plein S, Higgins DM, et al. Human myocardium: single-breath-hold MR T1 mapping with high spatial resolution-reproducibility study. Radiology 2006; 238(3):1004–1012.

30. Lee JJ, Liu S, Nacif MS, et al. Myocardial T1 and extracellular volume fraction mapping at 3 tesla. J Cardiovasc Magn Reson 2011;13(1):75.

31. Piechnik SK, Ferreira VM, Lewandowski AJ, et al. Normal variation of magnetic resonance T1 relaxation times in the human population at 1.5 T using ShMOLLI. J Cardiovasc Magn Reson 2013;15(1):13.

32. Salerno M, Janardhanan R, Jiji RS, et al. Comparison of methods for determining the partition coefficient of gadolinium in the myocardium using T1 mapping. J Magn Reson Imaging 2013;38(1):217–224.

33. Dabir D, Child N, Kalra A, et al. Reference values for healthy human myocardium using a T1 mapping methodology: results from the International T1 Multicenter Cardiovascular Magnetic Resonance study. J Cardiovasc Magn Reson 2014;16:69.

34. Liu CY, Liu YC, Wu C, et al. Evaluation of age-related interstitial myocardial fibrosis with cardiac magnetic resonance contrast-enhanced T1 mapping: MESA (Multi-Ethnic Study of Atherosclerosis). J Am Coll Cardiol 2013;62(14):1280–1287.

35. Chin CW, Semple S, Malley T, et al. Optimization and comparison of myocardial T1 techniques at 3T in patients with aortic stenosis. Eur Heart J Cardiovasc Imaging 2014;15(5):556–565.

36. Messroghli DR, Rudolph A, Abdel-Aty H, et al. An open-source software tool for the generation of relaxation time maps in magnetic resonance imaging. BMC Med Imaging 2010;10:16.

37. Kellman P, Wilson JR, Xue H, Ugander M, Arai AE. Extracellular volume fraction mapping in the myocardium, part 1: evaluation of an automated method. J Cardiovasc Magn Reson 2012;14:63.

38. Higgins DM, Ridgway JP, Radjenovic A, Sivananthan UM, Smith MA. T1 measurement using a short acquisition period for quantitative cardiac applications. Med Phys 2005;32(6):1738–1746.

39. Weingärtner S, Akçakaya M, Basha T, et al. Combined saturation/inversion recovery sequences for improved evaluation of scar and diffuse fibrosis in patients with arrhythmia or heart rate variability. Magn Reson Med 2014;71(3):1024–1034.

40. Roujol S, Weingärtner S, Foppa M, et al. Accuracy, precision, and reproducibility of four T1 mapping sequences: a head-to-head comparison of MOLLI, ShMOLLI, SASHA, and SAPPHIRE. Radiology 2014; 272(3):683–689.

41. Higgins CB, Herfkens R, Lipton MJ, et al. Nuclear magnetic resonance imaging of acute myocardial infarction in dogs: alterations in magnetic relaxation times. Am J Cardiol 1983;52(1):184–188.

42. Pflugfelder PW, Wisenberg G, Prato FS, Turner KL, Carroll SE. Serial imaging of canine myocardial infarction by in vivo nuclear magnetic resonance. J Am Coll Cardiol 1986;7(4):843–849.

43. Ugander M, Bagi PS, Oki AJ, et al. Myocardial edema as detected by pre-contrast T1 and T2 CMR delineates area at risk associated with acute myocardial infarction. JACC Cardiovasc Imaging 2012;5(6): 596–603.

44. Abdel-Aty H, Zagrosek A, Schulz-Menger J, et al. Delayed enhancement and T2-weighted cardiovascular magnetic resonance imaging differentiate acute from chronic myocardial infarction. Circulation 2004;109(20): 2411–2416.

45. Simonetti OP, Finn JP, White RD, Laub G, Henry DA. "Black blood" T2-weighted inversion-recovery MR imaging of the heart. Radiology 1996;199(1):49–57.

46. O h-Ici D, Ridgway JP, Kuehne T, et al. Cardiovascular magnetic resonance of myocardial edema using a short inversion time inversion recovery (STIR) black-blood technique: diagnostic accuracy of visual and semi-quantitative assessment. J Cardiovasc Magn Reson 2012;14:22.

47. Messroghli DR, Walters K, Plein S, et al. Myocardial T1 mapping: application to patients with acute and chronic myocardial infarction. Magn Reson Med 2007;58(1): 34–40.

48. Yilmaz A, Kindermann I, Kindermann M, et al. Comparative evaluation of left and right endomyocardial biopsy: differences in complication rate and diagnostic performance. Circulation 2010; 122(9):900–909.

49. Ferreira VM, Piechnik SK, Dall'Armellina E, et al. T(1) mapping for the diagnosis of acute myocarditis using CMR: comparison to T2-weighted and late gadolinium enhanced imaging. JACC Cardiovasc Imaging 2013;6(10):1048–1058.

50. Ferreira VM, Piechnik SK, Dall'Armellina E, et al. Native T1-mapping detects the location, extent and patterns of acute myocarditis without the need for gadolinium contrast agents. J Cardiovasc Magn Reson 2014;16:36.

51. Luetkens JA, Homsi R, Sprinkart AM, et al. Incremental value of quantitative CMR including parametric mapping for the diagnosis of acute myocarditis. Eur Heart J Cardiovasc Imaging 2015 Oct 16. [Epub ahead of print]

52. Hinojar R, Foote L, Arroyo Ucar E, et al. Native T1 in discrimination of acute and convalescent stages in patients with clinical diagnosis of myocarditis: a proposed diagnostic algorithm using CMR. JACC Cardiovasc Imaging 2015;8(1):37–46.

53. Puntmann VO, D'Cruz D, Smith Z, et al. Native myocardial T1 mapping by cardiovascular magnetic resonance imaging in subclinical cardiomyopathy in patients with systemic lupus erythematosus. Circ Cardiovasc Imaging 2013;6(2):295–301.

54. Ntusi NA, Piechnik SK, Francis JM, et al. Subclinical myocardial inflammation and diffuse fibrosis are common in systemic sclerosis--a clinical study using myocardial T1-mapping and extracellular volume quantification. J Cardiovasc Magn Reson 2014;16(1):21.

55. Ntusi NA, Piechnik SK, Francis JM, et al. Diffuse myocardial fibrosis and inflammation in rheumatoid arthritis: insights from CMR T1 mapping. JACC Cardiovasc Imaging 2015;8(5):526–536.

56. Wisenberg G, Pflugfelder PW, Kostuk WJ, McKenzie FN, Prato FS. Diagnostic applicability of magnetic resonance imaging in assessing human cardiac allograft rejection. Am J Cardiol 1987;60(1):130–136.

57. Miller CA, Naish JH, Shaw SM, et al. Multiparametric cardiovascular magnetic resonance surveillance of acute cardiac allograft rejection and characterisation of transplantation-associated myocardial injury: a pilot study. J Cardiovasc Magn Reson 2014;16(1):52.

58. Hosch W, Bock M, Libicher M, et al. MR-relaxometry of myocardial tissue: significant elevation of T1 and T2 relaxation times in cardiac amyloidosis. Invest Radiol 2007;42(9):636–642.

59. Maceira AM, Joshi J, Prasad SK, et al. Cardiovascular magnetic resonance in cardiac amyloidosis. Circulation 2005;111(2):186–193.

60. Karamitsos TD, Piechnik SK, Banypersad SM, et al. Noncontrast T1 mapping for the diagnosis of cardiac amyloidosis. JACC Cardiovasc Imaging 2013;6(4):488–497.

61. Fontana M, Banypersad SM, Treibel TA, et al. Native T1 mapping in transthyretin amyloidosis. JACC Cardiovasc Imaging 2014; 7(2):157–165.

62. Sado DM, White SK, Piechnik SK, et al. Identification and assessment of Anderson-Fabry disease by cardiovascular magnetic resonance noncontrast myocardial T1 mapping. Circ Cardiovasc Imaging 2013; 6(3):392–398.

63. Thompson RB, Chow K, Khan A, et al. T1 mapping with cardiovascular MRI is highly sensitive for Fabry disease independent of hypertrophy and sex. Circ Cardiovasc Imaging 2013;6(5):637–645.

64. Anderson LJ, Holden S, Davis B, et al. Cardiovascular T2-star (T2*) magnetic resonance for the early diagnosis of myocardial iron overload. Eur Heart J 2001;22(23):2171–2179.

65. Westwood MA, Anderson LJ, Firmin DN, et al. Interscanner reproducibility of cardiovascular magnetic resonance T2* measurements of tissue iron in thalassemia. J Magn Reson Imaging 2003;18(5):616–620.

66. Kirk P, Roughton M, Porter JB, et al. Cardiac T2* magnetic resonance for prediction of cardiac complications in thalassemia major. Circulation 2009;120(20):1961–1968.

67. Pennell DJ, Udelson JE, Arai AE, et al. Cardiovascular function and treatment in β-thalassemia major: a consensus statement from the American Heart Association. Circulation 2013;128(3):281–308. [Published correction appears in Circulation 2013; 128(13):e203.]

68. Feng Y, He T, Carpenter JP, et al. In vivo comparison of myocardial T1 with T2 and T2* in thalassaemia major. J Magn Reson Imaging 2013;38(3):588–593.

69. Sado DM, Maestrini V, Piechnik SK, et al. Noncontrast myocardial T1 mapping using cardiovascular magnetic resonance for iron overload. J Magn Reson Imaging 2015; 41(6):1505–1511.

70. Bull S, White SK, Piechnik SK, et al. Human non-contrast T1 values and correlation with histology in diffuse fibrosis. Heart 2013;99(13):932–937.

71. Sparrow P, Messroghli DR, Reid S, Ridgway JP, Bainbridge G, Sivananthan MU. Myocardial T1 mapping for detection of left ventricular myocardial fibrosis in chronic aortic regurgitation: pilot study. AJR Am J Roentgenol 2006;187(6):W630–W635.

72. Dass S, Suttie JJ, Piechnik SK, et al. Myocardial tissue characterization using magnetic resonance noncontrast t1 mapping in hypertrophic and dilated cardiomyopathy. Circ Cardiovasc Imaging 2012;5(6):726–733.

73. Puntmann VO, Voigt T, Chen Z, et al. Native T1 mapping in differentiation of normal myocardium from diffuse disease in hypertrophic and dilated cardiomyopathy. JACC Cardiovasc Imaging 2013;6(4):475–484.

74. Wong TC. Cardiovascular magnetic resonance imaging of myocardial interstitial expansion in hypertrophic cardiomyopathy. Curr Cardiovasc Imaging Rep 2014;7:9267.

75. Lee SP, Lee W, Lee JM, et al. Assessment of diffuse myocardial fibrosis by using MR imaging in asymptomatic patients with aortic stenosis. Radiology 2015;274(2):359–369.

76. van Heerebeek L, Borbély A, Niessen HW, et al. Myocardial structure and function differ in systolic and diastolic heart failure. Circulation 2006;113(16):1966–1973.

77. Gulati A, Jabbour A, Ismail TF, et al. Association of fibrosis with mortality and sudden cardiac death in patients with nonischemic dilated cardiomyopathy. JAMA 2013; 309(9):896–908.

78. Kim RJ, Fieno DS, Parrish TB, et al. Relationship of MRI delayed contrast enhancement to irreversible injury, infarct age, and contractile function. Circulation 1999; 100(19):1992–2002.

79. Soriano CJ, Ridocci F, Estornell J, Jimenez J, Martinez V, De Velasco JA. Noninvasive diagnosis of coronary artery disease in patients with heart failure and systolic dysfunction of uncertain etiology, using late gadolinium-enhanced cardiovascular magnetic resonance. J Am Coll Cardiol 2005;45(5):743–748.

80. Beltrami CA, Finato N, Rocco M, et al. Structural basis of end-stage failure in ischemic cardiomyopathy in humans. Circulation 1994;89(1):151–163.

81. Schelbert EB, Fonarow GC, Bonow RO, Butler J, Gheorghiade M. Therapeutic targets in heart failure: refocusing on the myocardial interstitium. J Am Coll Cardiol 2014;63(21):2188–2198.

82. Wong TC, Piehler K, Meier CG, et al. Association between extracellular matrix expansion quantified by cardiovascular magnetic resonance and short-term mortality. Circulation 2012;126(10):1206–1216.

83. Wong TC, Piehler KM, Kang IA, et al. Myocardial extracellular volume fraction quantified by cardiovascular magnetic resonance is increased in diabetes and associ-

ated with mortality and incident heart failure admission. Eur Heart J 2014;35(10): 657–664.

84. van Hoeven KH, Factor SM. A comparison of the pathological spectrum of hypertensive, diabetic, and hypertensive-diabetic heart disease. Circulation 1990;82(3):848–855.

85. Beltrami CA, Finato N, Rocco M, et al. The cellular basis of dilated cardiomyopathy in humans. J Mol Cell Cardiol 1995;27(1): 291–305.

86. Tamarappoo BK, John BT, Reinier K, et al. Vulnerable myocardial interstitium in patients with isolated left ventricular hypertrophy and sudden cardiac death: a postmortem histological evaluation. J Am Heart Assoc 2012;1(3):e001511.

87. Tanaka M, Fujiwara H, Onodera T, Wu DJ, Hamashima Y, Kawai C. Quantitative analysis of myocardial fibrosis in normals, hypertensive hearts, and hypertrophic cardiomyopathy. Br Heart J 1986;55(6): 575–581.

88. Rossi MA. Pathologic fibrosis and connective tissue matrix in left ventricular hypertrophy due to chronic arterial hypertension in humans. J Hypertens 1998;16(7): 1031–1041.

89. Flett AS, Sado DM, Quarta G, et al. Diffuse myocardial fibrosis in severe aortic stenosis: an equilibrium contrast cardiovascular magnetic resonance study. Eur Heart J Cardiovasc Imaging 2012;13(10):819–826.

90. Thum T, Gross C, Fiedler J, et al. MicroRNA-21 contributes to myocardial disease by stimulating MAP kinase signalling in fibroblasts. Nature 2008;456(7224):980–984.

91. Banypersad SM, Moon JC, Whelan C, Hawkins PN, Wechalekar AD. Updates in cardiac amyloidosis: a review. J Am Heart Assoc 2012;1(2):e000364.

92. Kim RJ, Albert TS, Wible JH, et al. Performance of delayed-enhancement magnetic resonance imaging with gadoversetamide contrast for the detection and assessment of myocardial infarction: an international, multicenter, double-blinded, randomized trial. Circulation 2008;117(5):629–637.

93. Kim HW, Farzaneh-Far A, Kim RJ. Cardiovascular magnetic resonance in patients with myocardial infarction: current and emerging applications. J Am Coll Cardiol 2009;55(1):1–16.

94. Wong TC, Piehler KM, Zareba KM, et al. Myocardial damage detected by late gadolinium enhancement cardiovascular magnetic resonance is associated with subsequent hospitalization for heart failure. J Am Heart Assoc 2013;2(6):e000416.

95. Almehmadi F, Joncas SX, Nevis I, et al. Prevalence of myocardial fibrosis patterns in patients with systolic dysfunction: prognostic significance for the prediction of sudden cardiac arrest or appropriate implantable cardiac defibrillator therapy. Circ Cardiovasc Imaging 2014;7(4):593–600.

96. Assomull RG, Prasad SK, Lyne J, et al. Cardiovascular magnetic resonance, fibrosis, and prognosis in dilated cardiomyopathy. J Am Coll Cardiol 2006;48(10): 1977–1985.

97. Wu KC, Weiss RG, Thiemann DR, et al. Late gadolinium enhancement by cardiovascular magnetic resonance heralds an adverse prognosis in nonischemic cardiomyopathy. J Am Coll Cardiol 2008;51(25): 2414–2421.

98. Kellman P, Wilson JR, Xue H, et al. Extracellular volume fraction mapping in the myocardium, part 2: initial clinical experience. J Cardiovasc Magn Reson 2012;14:64.

99. Broberg CS, Chugh SS, Conklin C, Sahn DJ, Jerosch-Herold M. Quantification of diffuse myocardial fibrosis and its association with myocardial dysfunction in congenital heart disease. Circ Cardiovasc Imaging 2010;3(6):727–734.

100. Schalla S, Bekkers SC, Dennert R, et al. Replacement and reactive myocardial fibrosis in idiopathic dilated cardiomyopathy: comparison of magnetic resonance imaging with right ventricular biopsy. Eur J Heart Fail 2010;12(3):227–231.

101. Doltra A, Messroghli D, Stawowy P, et al. Potential reduction of interstitial myocardial fibrosis with renal denervation. J Am Heart Assoc 2014;3(6):e001353.

102. Kawel N, Nacif M, Zavodni A, et al. T1 mapping of the myocardium: intra-individual assessment of the effect of field strength, cardiac cycle and variation by myocardial region. J Cardiovasc Magn Reson 2012;14:27.

103. McDiarmid AK, Swoboda PP, Erhayiem B, et al. Single bolus versus split dose gadolinium administration in extra-cellular volume calculation at 3 Tesla. J Cardiovasc Magn Reson 2015;17(1):6.

104. Liu S, Han J, Nacif MS, et al. Diffuse myocardial fibrosis evaluation using cardiac magnetic resonance T1 mapping: sample size considerations for clinical trials. J Cardiovasc Magn Reson 2012;14:90.

105. Edwards NC, Moody WE, Yuan M, et al. Quantification of left ventricular interstitial fibrosis in asymptomatic chronic primary degenerative mitral regurgitation. Circ Cardiovasc Imaging 2014;7(6):946–953.

106. Mehta BB, Chen X, Bilchick KC, Salerno M, Epstein FH. Accelerated and navigator-gated look-locker imaging for cardiac t1 estimation (ANGIE): Development and application to T1 mapping of the right ventricle. Magn Reson Med 2015;73(1): 150–160.

107. Mongeon FP, Jerosch-Herold M, Coelho-Filho OR, Blankstein R, Falk RH, Kwong RY. Quantification of extracellular matrix expansion by CMR in infiltrative heart disease. JACC Cardiovasc Imaging 2012; 5(9):897–907.

108. Robbers LF, Baars EN, Brouwer WP, et al. T1 mapping shows increased extracellular matrix size in the myocardium due to amyloid depositions. Circ Cardiovasc Imaging 2012;5(3):423–426.

109. Zhang S, Liu X, Bawa-Khalfe T, et al. Identification of the molecular basis of doxorubicin-induced cardiotoxicity. Nat Med 2012; 18(11):1639–1642.

110. Wassmuth R, Lentzsch S, Erdbruegger U, et al. Subclinical cardiotoxic effects of anthracyclines as assessed by magnetic resonance imaging-a pilot study. Am Heart J 2001;141(6):1007–1013.

111. Tham EB, Haykowsky MJ, Chow K, et al. Diffuse myocardial fibrosis by T1-mapping in children with subclinical anthracycline cardiotoxicity: relationship to exercise capacity, cumulative dose and remodeling. J Cardiovasc Magn Reson 2013;15:48.

112. Neilan TG, Coelho-Filho OR, Shah RV, et al. Myocardial extracellular volume by cardiac magnetic resonance imaging in patients treated with anthracycline-based chemotherapy. Am J Cardiol 2013;111(5): 717–722.

113. Radunski UK, Lund GK, Stehning C, et al. CMR in patients with severe myocarditis: diagnostic value of quantitative tissue markers including extracellular volume imaging. JACC Cardiovasc Imaging 2014;7(7): 667–675.

114. Schaper J, Mollnau H, Hein S, Scholz D, Münkel B, Devaux B. Interactions between cardiomyocytes and extracellular matrix in the failing human heart [in German]. Z Kardiol 1995;84(Suppl 4):33–38.

115. Khavandi K, Khavandi A, Asghar O, et al. Diabetic cardiomyopathy--a distinct disease? Best Pract Res Clin Endocrinol Metab 2009;23(3):347–360.

116. Asbun J, Villarreal FJ. The pathogenesis of myocardial fibrosis in the setting of diabetic cardiomyopathy. J Am Coll Cardiol 2006;47(4):693–700.

117. Puntmann VO, Voigt T, Chen Z, et al. Native T1 mapping in differentiation of normal myocardium from diffuse disease in hyper-

trophic and dilated cardiomyopathy. JACC Cardiovasc Imaging 2013;6(4):475–484.

118. Su MY, Lin LY, Tseng YH, et al. CMR-verified diffuse myocardial fibrosis is associated with diastolic dysfunction in HFpEF. JACC Cardiovasc Imaging 2014;7(10):991–997.

119. Schelbert EB, Piehler KM, Zareba KM, et al. Extracellular matrix expansion in non-infarcted myocardium is associated with subsequent death, hospitalization for heart failure, or both across the ejection fraction spectrum [abstr]. J Am Coll Cardiol 2014;63(12 Suppl):A1007.

120. McLenachan JM, Dargie HJ. Ventricular arrhythmias in hypertensive left ventricular hypertrophy. Relationship to coronary artery disease, left ventricular dysfunction, and myocardial fibrosis. Am J Hypertens 1990;3(10):735–740.

121. Kawara T, Derksen R, de Groot JR, et al. Activation delay after premature stimulation in chronically diseased human myocardium relates to the architecture of interstitial fibrosis. Circulation 2001;104(25):3069–3075.

122. Anderson KP, Walker R, Urie P, Ershler PR, Lux RL, Karwandee SV. Myocardial electrical propagation in patients with idiopathic dilated cardiomyopathy. J Clin Invest 1993;92(1):122–140.

123. Schwartzkopff B, Brehm M, Mundhenke M, Strauer BE. Repair of coronary arterioles after treatment with perindopril in hypertensive heart disease. Hypertension 2000;36(2):220–225.

124. Díez J, Querejeta R, López B, González A, Larman M, Martínez Ubago JL. Losartan-dependent regression of myocardial fibrosis is associated with reduction of left ventricular chamber stiffness in hypertensive patients. Circulation 2002;105(21):2512–2517.

125. Izawa H, Murohara T, Nagata K, et al. Mineralocorticoid receptor antagonism ameliorates left ventricular diastolic dysfunction and myocardial fibrosis in mildly symptomatic patients with idiopathic dilated cardiomyopathy: a pilot study. Circulation 2005;112(19):2940–2945.

126. Brilla CG, Funck RC, Rupp H. Lisinopril-mediated regression of myocardial fibrosis in patients with hypertensive heart disease. Circulation 2000;102(12):1388–1393.

127. Yusuf S, Sleight P, Pogue J, Bosch J, Davies R, Dagenais G. Effects of an angiotensin-converting-enzyme inhibitor, ramipril, on cardiovascular events in high-risk patients. The Heart Outcomes Prevention Evaluation Study Investigators. N Engl J Med 2000;342(3):145–153.

128. Effect of enalapril on survival in patients with reduced left ventricular ejection fractions and congestive heart failure. The SOLVD Investigators. N Engl J Med 1991;325(5):293–302.

129. Zannad F, Alla F, Dousset B, Perez A, Pitt B. Limitation of excessive extracellular matrix turnover may contribute to survival benefit of spironolactone therapy in patients with congestive heart failure: insights from the randomized aldactone evaluation study (RALES). Rales Investigators. Circulation 2000;102(22):2700–2706. [Published correction appears in Circulation 2001;103(3):476.]

130. Pfeffer MA, Braunwald E, Moyé LA, et al. Effect of captopril on mortality and morbidity in patients with left ventricular dysfunction after myocardial infarction. Results of the survival and ventricular enlargement trial. The SAVE Investigators. N Engl J Med 1992;327(10):669–677.

131. Pitt B, Zannad F, Remme WJ, et al. The effect of spironolactone on morbidity and mortality in patients with severe heart failure. Randomized Aldactone Evaluation Study Investigators. N Engl J Med 1999;341(10):709–717.

132. Pitt B, Remme W, Zannad F, et al. Eplerenone, a selective aldosterone blocker, in patients with left ventricular dysfunction after myocardial infarction. N Engl J Med 2003;348(14):1309–1321.

133. Pfeffer MA, McMurray JJ, Velazquez EJ, et al. Valsartan, captopril, or both in myocardial infarction complicated by heart failure, left ventricular dysfunction, or both. N Engl J Med 2003;349(20):1893–1906.

134. Kellman P, Arai AE, Xue H. T1 and extracellular volume mapping in the heart: estimation of error maps and the influence of noise on precision. J Cardiovasc Magn Reson 2013;15:56.

135. Kellman P, Herzka DA, Arai AE, Hansen MS. Influence of Off-resonance in myocardial T1-mapping using SSFP based MOLLI method. J Cardiovasc Magn Reson 2013;15:63.

136. Naghavi M, Libby P, Falk E, et al. From vulnerable plaque to vulnerable patient: a call for new definitions and risk assessment strategies. Part I. Circulation 2003;108(14):1164–1172.